Undulatory locomotion of *C. elegans* on wet surfaces: supporting material

X. N. Shen[1], J. Sznitman[2], P. Krajacic[3], T. Lamitina[3], and P. E. Arratia[1]

[1]Department of Mechanical Engineering and Applied Mechanics, University of Pennsylvania, Philadelphia, PA 19104, USA

[2]Department of Biomedical Engineering, Technion - Israel Institute of Technology, Technion City, Haifa 32000, Israel

[3]Department of Physiology, University of Pennsylvania, Philadelphia, PA 19104, USA

C. elegans strains, plate preparations and recordings

Wild type N2 (Bristol) worms were maintained using standard culture methods and fed with the *Escherichia coli* strain OP50. Analyses were performed on hypochlorite-synchronized young adult animals grown at 25°C. Agar plates were placed in the fumehood for 30 minutes to remove excessive moisture on agar surfaces. Worms were transferred to 6 cm NGM plates with no food 2 minutes before recording. Recordings of *C. elegans* crawling were obtained using a Leica MZ16FA microscope equipped with a Leica DFC 340 FX camera at 15 fps. The N2 strain was obtained from the *Caenorhabditis elegans* Genetic Stock Center (CGC).

Groove shape measurement using optical interferometer

We transfer one nematode *C. elegans* onto an agar plate. After 10 minutes, measurements of the groove shape left by the crawling nematode are conducted with a Zygo NewView 6300 Interferometer. This device scans the agar surface with white light, and has a sub-micron lateral resolution with a single nanometer height resolution. We use 20× external objectives for such measurements. The groove width varies from 26 to 30 μm and the depth of the groove ranges from 0.9 to 1.2 μm. For our analysis, we assume the groove is 1.0 μm deep and 28 μm wide, which are the mean values from the experiments (Fig. S1).

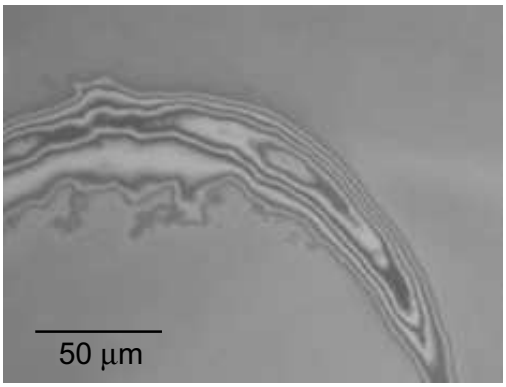

Figure S1: Optical interference patterns formed on an agar plate. The optical interference patterns are used to measure the depth and width of the groove.

Formulation of the lubrication equations

In this section, we derive the governing equations for the lubrication flow between the nematode and the substrate. We begin by formulating the continuity and momentum equations, in cylindrical coordinates for an incompressible two-dimensional (2D) fluid in the absence of body forces:

$$\frac{1}{r}\frac{\partial(ru_r)}{\partial r}+\frac{1}{r}\frac{\partial u_\theta}{\partial \theta} = 0, \tag{S1}$$

$$\frac{\partial u_r}{\partial t}+u_r\frac{\partial u_r}{\partial r}+\frac{u_\theta}{r}\frac{\partial u_r}{\partial \theta}-\frac{u_\theta^2}{r} = -\frac{1}{\rho}\frac{\partial p}{\partial r}+\frac{\mu}{\rho}\left(\nabla^2 u_r-\frac{u_r}{r^2}-\frac{2}{r^2}\frac{\partial u_\theta}{\partial \theta}\right), \tag{S2}$$

$$\frac{\partial u_\theta}{\partial t}+u_r\frac{\partial u_\theta}{\partial r}+\frac{u_\theta}{r}\frac{\partial u_\theta}{\partial \theta}+\frac{u_r u_\theta}{r} = -\frac{1}{\rho r}\frac{\partial p}{\partial \theta}+\frac{\mu}{\rho}\left(\nabla^2 u_\theta+\frac{2}{r^2}\frac{\partial u_r}{\partial \theta}-\frac{u_\theta}{r^2}\right). \tag{S3}$$

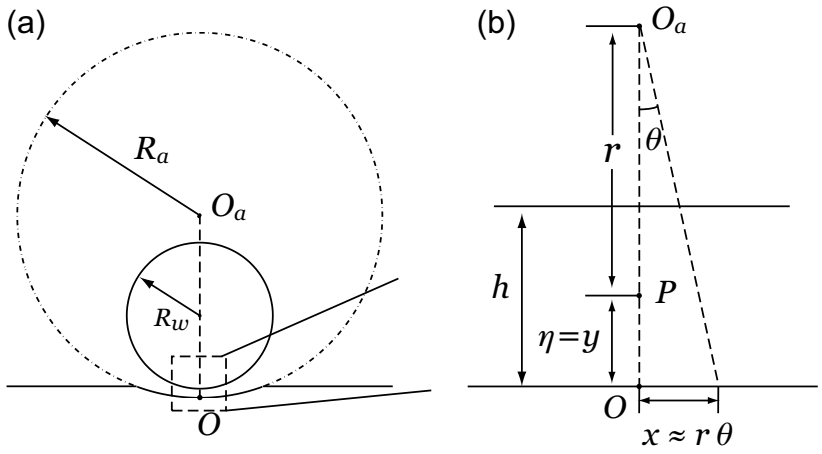

Figure S2: Schematic diagram of nematode cross-section and groove. (a) The radius of the nematode cross section and groove are R_w and R_a, respectively. The center of the groove is O_a and the middle point of the groove arc is O. (b) Detailed illustration of the dashed box shown in (a). The liquid film thickness is h. The distance from O_a to the position P in the liquid film is r, such that $\eta = R_a - r$. The x-y coordinate is defined as $x \approx r\theta$ and $y = \eta$ with its origin sitting on O.

Here, the two-dimensional velocity field $\mathbf{u}$ is described by its radial (u_r) and circumferential (u_θ) components. The fluid pressure is p, and the fluid density and viscosity are ρ and μ, respectively. In Fig. S2(a), cross-section profiles of the nematode body and the groove are shown. The radius of the groove and the nematode body are R_a and R_w, respectively. The origin of the cylindrical coordinate system is set at O_a. A detailed illustration of the thin liquid film is shown in Fig. S2(b), where the liquid thickness is $h = R_a - R_w$. The radial distance from the origin O_a to the position P in the liquid film is r. The distance from P to the groove center O is $\eta = R_a - r$. We introduce the following scalings,

$$\eta^* = \eta/h, \qquad r^* = r/R_a, \quad t^* = t/\tau,$$
$$u_r^* = u_r/(\delta v_n), \quad u_\theta^* = u_\theta/v_n, \quad p^* = p/(\mu v_n/\delta h),$$

where the characteristic speed v_n is the nematode normal crawling speed (see main article). The characteristic time is given by $\tau = R_a/v_n$. Here, the scalings for u_r^* and p^* are obtained by balancing the continuity and momentum equations. The liquid film is $O(1)$ μm, and $R_a = 100\mu$m. The normalized liquid film thickness is $\delta = h/R_a \ll 1$. We also note that $r^* = 1 - \delta(1-\eta) = 1 + O(\delta)$, such that $1/r^* = 1 + O(\delta)$. Following our scaling definitions, the momentum and continuity

equations in cylindrical coordinate are rewritten as,

$$\frac{\delta u}{R_a r^*}\frac{\partial (r^* u_r^*)}{\partial r} + \frac{u}{R_a r^*}\frac{\partial u_\theta^*}{\partial \theta} = 0, \tag{S4}$$

$$\frac{\delta u^2}{R_a}\frac{\partial u_r^*}{\partial t^*} + \frac{(\delta u)^2 u_r^*}{R_a}\frac{\partial u_r^*}{\partial r^*} + \frac{\delta u^2 u_\theta^*}{R_a r^*}\frac{\partial u_r^*}{\partial \theta} - \frac{u^2}{R_a}\frac{(u_\theta^*)^2}{r^*} = \tag{S5}$$

$$-\frac{\mu u}{\rho h^2}\frac{\partial p^*}{\partial r^*} + \frac{\mu}{\rho}\left[\frac{\delta u}{R_a^2 r^*}\frac{\partial}{\partial r^*}\left(r^*\frac{\partial u_r^*}{\partial r^*}\right) + \frac{\delta u}{R_a^2 r^{*2}}\frac{\partial^2 u_r^*}{\partial \theta^2} - \frac{\delta u}{R_a^2}\frac{u_r^*}{r^{*2}} - \frac{2u}{R_a^2 r^{*2}}\frac{\partial u_\theta^*}{\partial \theta}\right],$$

$$\frac{u^2}{R_a}\frac{\partial u_\theta^*}{\partial t} + \frac{\delta u^2 u^*}{R_a}\frac{\partial u_\theta^*}{\partial r^*} + \frac{u^2 u_\theta^*}{R_a r^*}\frac{\partial u_\theta^*}{\partial \theta} + \frac{\delta u^2}{R_a}\frac{u_\theta^* u_r^*}{r^*} = \tag{S6}$$

$$-\frac{\mu u}{\rho h^2 r^*}\frac{\partial p^*}{\partial \theta} + \frac{\mu}{\rho}\left[\frac{u}{R_a^2 r^*}\frac{\partial}{\partial r^*}\left(r^*\frac{\partial u_\theta^*}{\partial r^*}\right) + \frac{u}{R_a^2 r^{*2}}\frac{\partial^2 u_\theta^*}{\partial \theta^2} + \frac{2\delta u}{R_a^2 r^{*2}}\frac{\partial u_r^*}{\partial \theta} - \frac{u}{R_a^2}\frac{u_\theta^*}{r^{*2}}\right].$$

The radial distance r is related to η by $\eta = R_a - r$. Thus $\partial/\partial r = -\partial/\partial\eta$. Following our scaling choice, $\partial/\partial r^* = -\partial/(\delta\partial\eta^*)$. We use the relationship between r and η and rearrange Eqs. 4–6 to obtain,

$$\frac{\partial p^*}{\partial \eta^*} + O(\delta^2, \delta^3 Re) = 0, \tag{S7}$$

$$\frac{\partial p^*}{\partial \theta} - \frac{\partial^2 u_\theta^*}{\partial \eta^{*2}} + O(\delta, \delta Re) = 0, \tag{S8}$$

$$\frac{\partial u_r^*}{\partial \eta^*} - \frac{\partial u_\theta^*}{\partial \theta} + O(\delta) = 0. \tag{S9}$$

The nematode's typical normal sliding speed v_n is 1 mm/s (experimentally measured), and the viscosity and density of the liquid are $\mu = 10$ mPa s and $\rho = 10^3$ kg/m^3, respectively. The liquid film thickness is h $\approx$ 1 μm (1). Here, the Reynolds number is defined as $Re = 2\rho v_n\sqrt{2R_a h}/\mu \approx 3\times10^{-3}$, and the dimensionless gap width $\delta = h/R_a \approx 0.01$. We neglect terms smaller than or equal to $O(\delta)$ and $O(\delta Re)$ such that,

$$\frac{\partial p^*}{\partial \eta^*} = 0, \tag{S10}$$

$$\frac{\partial p^*}{\partial \theta} - \frac{\partial^2 u_\theta^*}{\partial \eta^{*2}} = 0, \tag{S11}$$

$$\frac{\partial u_r^*}{\partial \eta^*} - \frac{\partial u_\theta^*}{\partial \theta} = 0. \tag{S12}$$

The simplified equations are rearranged into dimensional form to facilitate further computations,

$$\frac{\partial u_r}{\partial \eta} - \frac{\partial u_\theta}{r\partial \theta} = 0, \tag{S13}$$

$$\frac{\partial p}{\partial \eta} = 0, \tag{S14}$$

$$\frac{\partial p}{r\partial \theta} - \mu\frac{\partial^2 u_\theta}{\partial \eta^2} = 0. \tag{S15}$$

We see that in the lubrication regime, the effects of geometry curvature are negligible. Hence, we can rearrange and simplify Eqs. S13–S15 into Cartesian coordinates by writing $x = r\theta$ and $y = \eta$

such that,

$$\frac{\partial p}{\partial y} = 0, \tag{S16}$$

$$\frac{\partial p}{\partial x} - \mu \frac{\partial^2 u_x}{\partial y^2} = 0, \tag{S17}$$

$$\frac{\partial u_y}{\partial y} + \frac{\partial u_x}{\partial x} = 0. \tag{S18}$$

We note that $x = r\theta$ is an approximation to $x = r\sin\theta$, which yields an error less than $\delta/10$ as $|\theta| < |\theta_c|$. Since the nematode slides laterally along the surface with velocity v_n, the boundary conditions are:

$$\begin{array}{ll} u_x(y=0) = 0, & u_y(y=0) = 0, \\ u_x(y=h) = -v_n\cos\theta \approx -v_n, & u_y(y=0) = -v_n\sin\theta \approx -v_n\frac{dh}{dx}, \end{array}$$

where $\theta < 20^\circ$ (see main article). Integrating the lubrication equations with the appropriate boundary conditions yields the following velocity profiles for u_x and u_y :

$$u_x = \frac{1}{2\mu}\frac{\partial p}{\partial x}y^2 - \frac{1}{h}\left(v_n + \frac{h^2}{2\mu}\frac{\partial p}{\partial x}\right)y, \tag{S19}$$

$$u_y = -\frac{1}{6\mu}\frac{\partial^2 p}{\partial x^2}y^3 + \frac{1}{2}\frac{\partial}{\partial x}\left(\frac{h}{2\mu}\frac{\partial p}{\partial x}\right)y^2 - \frac{v_n}{2h^2}\frac{\partial h}{\partial x}y^2. \tag{S20}$$

Note that the expressions for u_x and u_y satisfy the first three boundary conditions. Using the last boundary condition ($u_y(y=h) = -v_n dh/dx$) yields the well-known Reynolds equation

$$\frac{\partial}{\partial x}\left(\frac{h^3}{12\mu}\frac{\partial p}{\partial x}\right) = -\frac{v_n}{2}\frac{dh}{dx}. \tag{S21}$$

The effect of surface tension on nematode crawling

Motility on agar surfaces and surfactant treated agar surfaces

The effect of the liquid meniscus attached to the nematode body and surface tension on undulatory locomotion on surfaces has been previously observed (2). To understand the effect of surface tension and related contact angle hysteresis on nematode crawling, we use the surfactant Tween 20 to alter the surface tension of the liquid film on the agar plate and the related contact angle hysteresis during crawling (3). Tween 20 is relatively non-toxic and has been previously used in bacteria swarming (4, 5) and *C. elegans* developmental studies (6). We prepared Tween 20 solutions in M9 buffer. The concentration of Tween 20 in M9 is 8×10^{-5} M (or approximately 0.1 g/L), which is the critical micelle concentration (cmc) of Tween 20 (7). We choose Tween 20 M9 solution at cmc to (i) maximize surface tension reduction (we note that surface tension reaches its minimum at cmc); (ii) mitigate the effect of surfactant on *C. elegans* motility.

In experiments, we spread 500 μL of Tween solution on top of an agar plate. The treated agar plate is then placed inside a fume hood for 30 minutes to remove excessive moisture. The resultant liquid / air surface tension of the film is approximately 38 mN/m (7), which is 50% smaller than for pure water ($\sim$71 mN/m). The effect of Tween 20 can be demonstrated by comparing the spreading

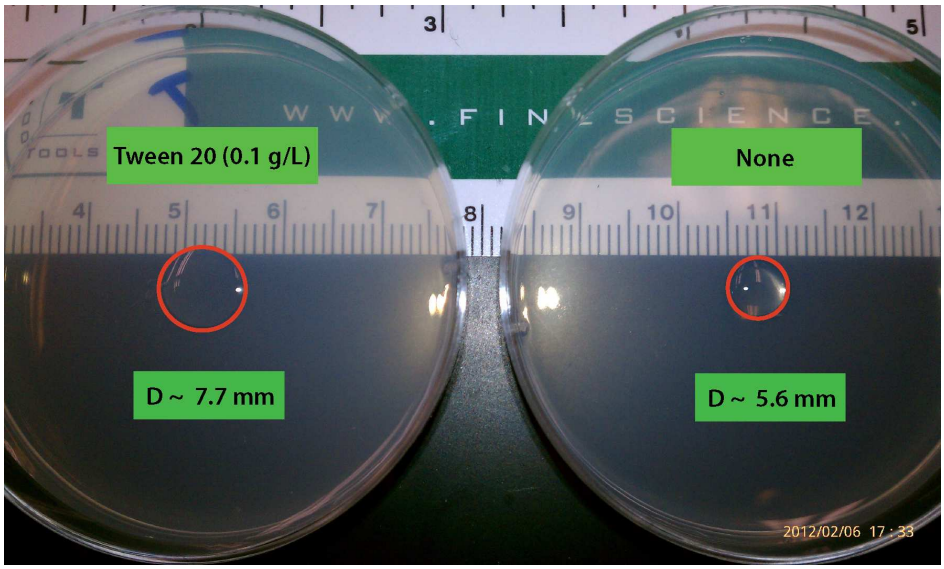

Figure S3: Demonstration of reduced surface tension with Tween 20. We placed 25 μL Halocarbon oil 27 on Tween 20 treated (left) and standard agar plates (right). The diameters of the drop are 7.7 mm and 5.6 mm, respectively.

radius of 25 μL oil drops (Halocarbon oil 27, Sigma-Aldrich) on a Tween 20 treated plate and a standard agar plate (See Figure S3). The larger spreading radius on Tween 20 treated agar plate is due to the reduced surface tension.

We record the motility of *C. elegans* under the same experimental setup described in the main text. Nematodes are recorded within 3 minutes after being placed on Tween 20 treated agar plates to minimize any effect of surfactant on the nematodes. A total of 14 worms were recorded on Tween 20 treated agar plates.

Theoretical estimates of surface tension forces

We also investigate the effects of asymmetric menisci (and surface tension) on nematode motility by studying the force balance on the nematode body. First, we model menisci surfaces as circular arcs of different radii (8). The spanning angles of the left and right meniscus (see Fig. S4), from the nematode body to the bottom liquid film, are denoted ϕ_1 and ϕ_2. The corresponding radii of curvature of the menisci are R_1 and R_2, respectively, and the contact angles are ψ_1 and ψ_2. The ambient pressure is $p = p_0$, while the pressure values at the left and right boundaries of the menisci are $p = p_1$ and $p = p_2$. Based on the geometries, we can show that $\phi_1 + \psi_1 + \theta_1 = \pi$ and $\phi_2 + \psi_2 + \theta_2 = \pi$, and the radii of curvature can be formulated as,

$$R_{1,2} = R_w \frac{1 - \cos\theta_{1,2}}{1 - \cos\phi_{1,2}} = R_w \frac{1 - \cos\theta_{1,2}}{1 + \cos(\psi_{1,2} + \theta_{1,2})}. \tag{S22}$$

Thus, the pressure differences Δp_1 and Δp_2 can be computed from the Young-Laplace equation,

$$\Delta p_{1,2} = p_{1,2} - p_0 = -\frac{\gamma}{R_{1,2}} = -\frac{\gamma}{R_w} \frac{1 + \cos(\psi_{1,2} + \theta_{1,2})}{1 - \cos\theta_{1,2}}. \tag{S23}$$

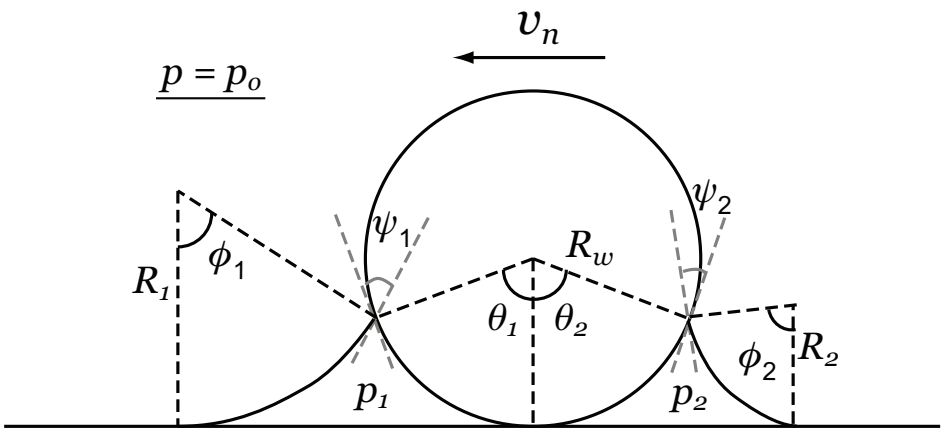

Figure S4: Schematic illustration of the liquid menisci attached to the nematode body.

The pressures of the liquid menisci are therefore

$$p_{1,2} = p_0 - \frac{\gamma}{R_{1,2}} = p_0 - \frac{\gamma}{R_w}\frac{1+\cos(\psi_{1,2}+\theta_{1,2})}{1-\cos\theta_{1,2}}. \tag{S24}$$

Given the pressure distribution on the two sides of nematode, we can now compute the surface tension force along the normal direction,

$$F_\gamma = \int_0^{\theta_1} p_1 \sin\theta \; R_w d\theta - \int_0^{\theta_2} p_2 \sin\theta \; R_w d\theta. \tag{S25}$$

Equation S25 can be integrated and simplified so that

$$F_\gamma = \gamma[\cos(\psi_2+\theta_2) - \cos(\psi_1+\theta_1)]. \tag{S26}$$

Since it is known that mucin-like glycoprotein fluid coats the nematode's cuticle (9) and that the interfacial tension between the liquid film and the mucin coating is very small (<1 mN/m) (10), we set the contact angles between the liquid film and the mucin coating $\psi_1 \approx \psi_2 \approx 0$. Hence, the resulting surface tension force is a function of surface tension γ and the angular span θ of the menisci so that

$$F_\gamma = \gamma(\cos\theta_2 - \cos\theta_1) = 2\gamma \sin\frac{\theta_1-\theta_2}{2}\sin\frac{\theta_1+\theta_2}{2}. \tag{S27}$$

Based on direct observations of meniscus spreading on agar surfaces, we set $\theta_1 = 55^\circ$ and $\theta_2 = 45^\circ$. These values are difficult to measure (11) and we only provide a rough estimate here. Because the value of θ_1 is larger than θ_2, F_γ opposes the normal (lateral) motion of the nematode (see Fig. 4). Note that $F_\gamma = 0$ for $\theta_1 = \theta_2$. Using Eq. S27, we compute the normal surface tension force F_γ to be approximately 0.67 mN/m. For comparison, the normal lubrication force is approximately 2.2 mN/m, where the liquid viscosity μ is 10 mPa s and normal (lateral) speed v_n is 1 mm/s. Surface tension force accounts for approximately 20% of the total propulsive force of a nematode during crawling. The experiments (See main text) and theoretical estimations provided suggest that surface tension plays a finite yet limited role on the motility kinematics and on the overall propulsion forces of *C. elegans* on agar plates. While the effects of surface tension on *C. elegans* motility warrant a more in-depth study, here we will focus our efforts on viscous lubrication forces which seem to be the dominant component.

The drag force on the nematode body due to lateral motions

We approximate the outer and inner cylinders with profiles $h_o = x^2/2R_a$ and $h_i = h_0 + x^2/2R_w$, respectively. Thus, the gap width follows as $h = h_i - h_o = h_0 + (1/2)(R_w^{-1} - R_a^{-1})x^2$. We introduce $C = (1/2)(R_w^{-1} - R_a^{-1})R_w^2$ and $e = h_0/C$ such that the gap width may be rewritten as $h = C(e+X^2)$, where $X = x/R_w$. We note that given the parabolic approximation, the characteristic length scale is $x = \sqrt{2R_w h}$. Since $\partial p/\partial y = 0$, the partial differential yields $\partial p/\partial x = dp/dx$, and the Reynolds equation can be rewritten as,

$$\frac{d}{dx}\left(\frac{h^3}{12\mu}\frac{dp}{dx}\right) = -\frac{v_n}{2}\frac{dh}{dx}. \tag{S28}$$

Since mucin-like glycoprotein fluid coats the nematode's cuticle (9, 12) which is partly miscible with water, we assume perfect wetting (i.e., $\theta_1 = \theta_2 = 0$). We estimate the film contact angle $\psi_1 = \psi_2 = \pi/4$ based on direct observations of meniscus spreading on agar surfaces. The radius of the nematode cross-section is $R_w = 40$ μm. The surface tension between the liquid menisci and air is set at a typical value of $\gamma = 5$ mN/m. The meniscus pressure is found to be $p_2 = -125$ Pa.

We integrate the Reynolds equation once,

$$\frac{dp}{dx} = -6\mu v_n \frac{h - h_m}{h^3}. \tag{S29}$$

The symmetry of the meniscus shapes gives boundary condition $dp/dx = 0$ at $x = x_m (X = X_m)$. Substituting the gap width profile, the Reynolds equation reduces to

$$\frac{dp}{dx} = -\frac{6\mu v_n}{C^2}\frac{X^2 - X_m^2}{(e+X^2)^3}. \tag{S30}$$

The pressure is then given by

$$\begin{aligned} p &= -\frac{6\mu v_n R_w}{C^2}\left(\int \frac{X^2}{(e+X^2)^3}dX - X_m^2 \int \frac{1}{(e+X^2)^3}dX\right) + D \\ &= -\frac{6\mu v_n R_w}{C^2}(J_1(e,X) - X_m^2 J_2(e,X)) + D, \end{aligned} \tag{S31}$$

$$J_1(e,X) \triangleq \int_0^X \frac{t^2}{(e+t^2)^3}dt, \tag{S32}$$

$$J_2(e,X) \triangleq \int_0^X \frac{1}{(e+t^2)^3}dt. \tag{S33}$$

The boundary condition $p = p_2$ at $X = X_m$ gives

$$D = \frac{6\mu v_n R_w}{C^2}(J_1(e,X_m) - X_m^2 J_2(e,X_m)) + p_2. \tag{S34}$$

We assume the fluid in the gap to be Newtonian such that the 2D stress tensor is given by

$$\boldsymbol{\tau} = -p\mathbf{I} + 2\mu\mathbf{D} = \begin{pmatrix} -p + 2\mu\frac{\partial u_x}{\partial x} & \mu(\frac{\partial u_y}{\partial x} + \frac{\partial u_x}{\partial y}) \\ \mu(\frac{\partial u_y}{\partial x} + \frac{\partial u_x}{\partial y}) & -p + 2\mu\frac{\partial u_y}{\partial y} \end{pmatrix}. \tag{S35}$$

The fluid drag force opposing sliding along the x-axis follows as

$$\begin{aligned} F_x(y=h) &= \int_S -\tau_{xx}|_{y=h}\sin\theta + \tau_{xy}|_{y=h}\cos\theta \; dS \\ &= \int_{-x_m}^{x_m}\left[\left(p - 2\mu\frac{\partial u_x}{\partial x}\right)\sin\theta + \mu\left(\frac{\partial u_y}{\partial x}+\frac{\partial u_x}{\partial y}\right)\cos\theta\right]dx \\ &\approx \int_{-x_m}^{x_m}\left[\left(p - 2\mu\frac{\partial u_x}{\partial x}\right)\frac{dh}{dx} + \mu\left(\frac{\partial u_y}{\partial x}+\frac{\partial u_x}{\partial y}\right)\right]dx \\ &= \underbrace{\int_{-x_m}^{x_m}\left[\left(p - 2\mu\frac{\partial u_x}{\partial x}\right)\right]dh}_{F_{x1}} + \underbrace{\int_{-x_m}^{x_m}\mu\left(\frac{\partial u_y}{\partial x}+\frac{\partial u_x}{\partial y}\right)dx}_{F_{x2}}. \end{aligned} \tag{S36}$$

In the above expression for $F_x(y=h)$, the contribution to lateral resistance arising from (i) the normal stress component (F_{x1}) and (ii) the shear stress component (F_{x2}) can be obtained by integrating separately each expression. By using the continuity statement ($\partial v_x/\partial x + \partial v_y/\partial y = 0$) and lubrication assumption of unidirectional flow $v_x \sim v_n$, we arrive at $v_y \sim v_n\sqrt{h/R_w}$. In the expression for F_{x1}, the normal expansion rate $\mu\partial u_x/\partial x$ is $O(\delta^{\frac{3}{2}})$ with respect to the pressure p ($\mu\partial u_x/\partial x \sim \mu v_n/\sqrt{2R_w h}$ and $p \sim \mu v_n/(\delta h)$). Similarly, in the expression for F_{x2}, the term $\partial u_y/\partial x$ is $O(\delta)$ with respect to $\partial u_x/\partial y$ ($\partial u_y/\partial x \sim v_n/R_w$ and $\partial u_x/\partial y \sim v_n/h$). We omit terms smaller than or equal to $O(\delta)$ and carry the integration. We note that $h = C(e+X^2)$ and $dh = 2CXdX$.

$$\begin{aligned} F_{x1} &\approx \int_{-x_m}^{x_m} p\; dh \\ &= -\frac{6\mu v_n R_w}{C^2}\left(\int_{-X_m}^{X_m} J_1(e,X)(2CXdX) - X_m^2\int_{-X_m}^{X_m} J_2(e,X)(2CXdX) + \int_{-X_m}^{X_m} D(2CXdX)\right) \\ &= -\frac{12\mu v_n R_w}{C}\left(\int_{-X_m}^{X_m} J_1(e,X)XdX - X_m^2\int_{-X_m}^{X_m} J_2(e,X)XdX\right) + 0 \\ &= \frac{3}{2}\frac{\mu v_n R_w}{C}\left[\left(3e^{-1/2} - 2X_m^2 e^{-3/2} + 3X_m^4 e^{-5/2}\right)\arctan\left(\frac{X_m}{\sqrt{e}}\right) - 3X_m e^{-1} + 3X_m^3 e^{-2}\right], \end{aligned} \tag{S37}$$

$$\begin{aligned} F_{x2} &\approx \int_{-x_m}^{x_m}\mu\frac{\partial u_x}{\partial y}dx \\ &= -\mu v_n\int_{-X_m}^{X_m}\frac{(4X^2 - 3X_m^2 + e)}{C(e+X^2)^2}R_w dX \\ &= \frac{\mu v_n R_w}{C}\left[\left(3X_m^2 e^{-3/2} - 5e^{-1/2}\right)\arctan\left(\frac{X_m}{\sqrt{e}}\right) + 3X_m e^{-1}\right]. \end{aligned} \tag{S38}$$

The total lateral resistance force follows as,

$$\begin{aligned} F_x &= F_{x1} + F_{x2} \\ &= \frac{\mu v_n R_w}{C}\left[\frac{9}{2}\arctan\left(\frac{X_m}{\sqrt{e}}\right)X_m^4 e^{-\frac{5}{2}} + \frac{9}{2}X_m^3 e^{-2} - \frac{3}{2}X_m e^{-1}\right. \\ &\qquad \left. -\frac{1}{2}\arctan\left(\frac{X_m}{\sqrt{e}}\right)e^{-\frac{1}{2}}\right]. \end{aligned} \tag{S39}$$

Similarly, the force supporting along y-axis F_y follows as

$$
\begin{aligned}
F_y(y=h) &= \int_S -\tau_{yx}|_{y=h}\sin\theta + \tau_{yy}|_{y=h}\cos\theta \; dS \qquad \text{(S40)}\\
&= \int_{-x_m}^{x_m}\left[-\mu\left(\frac{\partial u_y}{\partial x}+\frac{\partial u_x}{\partial y}\right)\sin\theta + \left(-p+2\mu\frac{\partial u_x}{\partial x}\right)\cos\theta\right]dx\\
&\approx \int_{-x_m}^{x_m}\left[\left(-\mu\frac{\partial u_x}{\partial y}\right)\frac{dh}{dx} - p\right]\; dx\\
&= \int_{-x_m}^{x_m}\left(-\mu\frac{\partial u_x}{\partial y}\right)dh - \int_{-x_m}^{x_m} p\; dx\\
&= 0+\frac{6\mu v_n R_w^2}{C^2}\left(\int_{-X_m}^{X_m} J_1(e,X)dX - X_m^2\int_{-X_m}^{X_m} J_2(e,X)dX\right) - 2Dx_m\\
&= 0+0-\left[12\mu v_n X_m(J_1(e,X_m)-X_m^2 J_2(e,X_m))\left(\frac{R_w}{C}\right)^2 + 2p_2x_m\right]\\
&= \left[\mu v_n\left(\frac{R_w}{C}\right)^2\right]\frac{3}{2}\frac{X_m}{e^{5/2}(e+X_m^2)}\left(3\arctan\left(\frac{X_m}{\sqrt{e}}\right)X_m^4 + 3\sqrt{e}X_m^3 + 2e\arctan\left(\frac{X_m}{\sqrt{e}}\right)X_m^2\right.\\
&\quad \left. + e^{3/2}X_m - e^2\arctan\left(\frac{X_m}{\sqrt{e}}\right)\right) + 2p_2x_m.
\end{aligned}
$$

The shape parameter is $C = 13.3$ μm and $X_m = \sin(\pi/12)$ (see main article). The gap width is $h_0 = 0.49\mu$m and $e = 0.04$. The vertical force $F_y(y=h) \approx 3591\mu v_n + 2p_2x_m$. The net resultant force has two parts, i.e., the lubrication support force ($F_{\text{lub}} = 3591\ \mu v_n$), and the capillary force ($F_{\text{cap}} = 2p_2x_m$ with $p_2 < 0$).

The normal sliding speed averaged along the nematode body is $v_n \approx 0.1$ mm/s. The fluid of viscosity $\mu = 10$ mPa·s, and the lubrication force $F_{\text{lub}} = 3.6\times10^{-3}$ N/m, while the capillary force yields $F_{\text{cap}} = -3.5\times10^{-3}$ N/m. The lubrication force and capillary force are approximately balanced ($F_y \approx 0$), sustaining a stable lubrication layer. We also note the gravity force is negligible in this situation since $G = \rho(\pi R_w^2)g = 5.0\times10^{-5}$ N/m. In sum, we see that the lubrication force is able to support the nematode body in the gravitational direction.

The drag force on the nematode body due to forward motion

In addition to lateral sliding in the direction normal to the nematode's longitudinal axis, the nematode crawls forward along the z-axis. Since $h \ll R_w$, the configuration is modeled as parallel shear between two infinite plates. The fluid drag force opposing motion in the z-axis is integrated from $-R_w\sin\theta_c$ to $R_w\sin\theta_c$,

$$
\begin{aligned}
F_z(y=h) &= -\int_S \mu\frac{v_t}{h}dx \qquad \text{(S41)}\\
&= -\int_{-\sin\theta_c}^{\sin\theta_c}\mu\frac{v_t}{C(e+X^2)}\; R_w dX\\
&= \mu v_t\frac{R_w}{C}\left(2\arctan\left(\frac{\sin\theta_c}{\sqrt{e}}\right)e^{-1/2}\right).
\end{aligned}
$$

As for a typical tangential crawling speed $v_t = 0.2$mm/s, the tangential drag force is $F_z = 6 \times 10^{-6}$ N/m.

The role of the groove in nematode crawling

As the nematode crawls on agar surfaces, it creates and leaves behind a trail of grooves. The generation of grooves could result from three forces: (a) forces due to surface tension, (b) forces from liquid lubrication (i.e. shearing) and (c) gravity force of the nematode body. We neglect gravity forces because they are two orders of magnitude smaller than surface tension or lubrication forces (see page 9 in supporting material). Lubrication forces, as a way of propulsion, are the main focus of this manuscript and are discussed in the main text. Here, we discuss forces due to surface tension.

Surface tension forces acting on the nematode can also create grooves. In order to demonstrate this process, we offer a simple estimation of the force necessary to deform an agar surface by a rigid cylinder. Using the Johnson-Kendall-Roberts (JKR) contact mechanics model (13), we find that an agar surface possessing a shear-modulus of 10^5 Pa can be deformed by 3 μm under the action of a surface tension force that is approximately 5×10^{-3} N/m. That is, the agar surface can easily be deformed by the action of surface tension between a cylinder and the liquid film. In our experiments, we estimate the gravitational force to be approximately 5×10^{-5} N/m and the surface tension to be 3.5×10^{-3} N/m in the gravitational direction. This surface tension force in along the gravitational direction does not produce propulsion but it can plastically deform the agar surface.

In additional to forces in the gravitational direction that produces no propulsion, the surface tension force can also act along the normal direction. This normal direction can create the groove and provide propulsion. However, we have shown that the normal (shear) component plays a small role in propulsion (see page 9 in main text, and page 6 under Eq. 27 in supporting material). We therefore do not consider the groove generating forces to be a major contributor to propulsion.

The computation of the bending force F_b

The nematode generates internal forces which bend its body to undulate and maintain its body length We note that the measured nematode body is of constant length (1.21±0.04 mm) during crawling (14, 15). By a force balance along the nematode body, the muscle force $\vec{F}$ can be expressed as following,

$$\vec{F}(s_p, t) = K_b \frac{\partial \kappa(s_p, t)}{\partial s} \vec{n}(s_p, t) + \mu \int_0^{s_p} C_n \vec{v}_n(s, t) + C_t \vec{v}_t(s, t)\ ds, \tag{S42}$$

where the first term represents the elastic force to bend the nematode body and the second term is the viscous drag force imposed by liquid film. The muscle force $\vec{F}$ is decomposed along the normal and tangential directions. The tangential component $F_t = \vec{F} \cdot \vec{t}$ maintains the body length, while the bending force (i.e., the normal component) $F_b = \vec{F} \cdot \vec{n}$ bends the nematode body.

The normal and tangential velocity vectors can be rearranged as $\vec{v}_t = v_t \vec{t}$ and $\vec{v}_n = v_n \vec{n}$. The

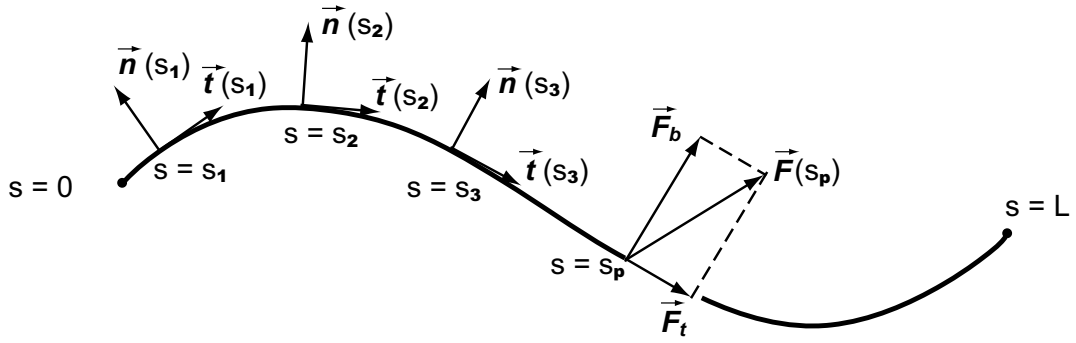

Figure S5: Illustration of the nematode geometry. Along the body from the head $s = 0$ to the tail $s = L$, at each position the unit normal and tangential vectors $\vec{n}$ and $\vec{t}$ are obtained. At the position $s = s_p$, the muscle force $\vec{F}(s_p)$ is decomposed along the normal and tangential directions. The tangential component $F_t = \vec{F} \cdot \vec{t}$ maintains the body length, and the bending force (i.e., the normal component) $F_b = \vec{F} \cdot \vec{n}$ bends the nematode body.

bending force F_b is therefore computed as

$$\begin{aligned} F_b(s_p,t) &= \vec{F}(s_p,t) \cdot \vec{n}(s_p,t) \\ &= K_b \frac{\partial \kappa(s_p,t)}{\partial s} \vec{n}(s_p,t) \cdot \vec{n}(s_p,t) + \mu \left(\int_0^{s_p} C_n \vec{v}_n(s,t) + C_t \vec{v}_t(s,t)\ ds \right) \cdot \vec{n}(s_p,t) \\ &= K_b \frac{\partial \kappa(s_p,t)}{\partial s} + \mu \int_0^{s_p} C_n\ v_n(s,t)\ \ [\vec{n}(s,t) \cdot \vec{n}(s_p,t)] + C_t\ v_t(s,t)\ \ \left[\vec{t}(s,t) \cdot \vec{n}(s_p,t)\right]\ ds. \end{aligned} \tag{S43}$$

Here, we note that due to the nature of the undulatory shape, $\vec{t}(s,t) \cdot \vec{n}(s_p,t)$ $(s \neq s_p)$ is usually non-zero, since each segment of the nematode body has a distinct orientation. The computation of the bending force incorporates both the elastic force part and the viscous force part. As shown in the text, the phase between the bending force F_b and the bending curvature κ changes as viscous drag forces vary.

Supporting references

1. Hamrock, B. J., S. R. Schmid, and B. O. Jacobson, 2004. Fundamentals of Fluid Film Lubrication. Marcel Dekker.

2. Wallace, H. R., 1958. Movement of eelworms. I. The influence of pore size and moisture content of the soil on the migration of larvae of the beet eelworm, *Heterodera schachtii Schmidt. Ann. Appl. Biol.* 46:74–85.

3. Eckmann, D. M., D. P. Cavanagh, and A. B. Branger, 2001. Wetting characteristics of aqueous surfactant-laden drops. *J. Colloid Interface Sci.* 242:386–394.

4. Guasto, J. S., K. A. Johnson, and J. P. Gollub, 2010. Oscillatory Flows Induced by Microorganisms Swimming in Two Dimensions. *Phys. Rev. Lett.* 105:168102.

5. Kurtuldu, H., J. S. Guasto, K. A. Johnson, and J. P. Gollub, 2011. Enhancement of biomixing by swimming algal cells in two-dimensional films. *Proc. Natl. Acad. Sci. U.S.A.* 108:10391–10395.

6. Mutwakil, M. H., T. J. Steele, K. C. Lowe, and D. I. de Pomerai, 1997. Surfactant stimulation of growth in the nematode *Caenorhabditis elegans*. *Enzyme Microb. Technol.* 20:462–470.

7. Kim, C., and Y.-L. Hsieh, 2001. Wetting and absorbency of nonionic surfactant solutions on cotton fabrics. *Colloids Surf., A* 187-188:385–397.

8. Gart, S., D. Vella, and S. Jung, 2011. The collective motion of nematodes in a thin liquid layer. *Soft Matter* 7:2444–2448.

9. Gems, D., and R. M. Maizels, 1996. An abundantly expressed mucin-like protein from Toxocara canis infective larvae: the precursor of the larval surface coat glycoproteins. *Proc. Natl. Acad. Sci. U.S.A.* 93:1665–1670.

10. Sharma, A., and E. Ruckenstein, 1986. The role of lipid abnormalities, aqueous and mucus deficiencies in the tear film breakup, and implications for tear substitutes and contact lens tolerance. *J. Colloid Interface Sci.* 111:8–34.

11. Sauvage, P. 2007. Study of the locomotion of *C. elegans* movement and mechanical perturbations. PhD thesis. Universite Paris Diderot-Paris 7, Paris .

12. Hemmer, R. M., S. G. Donkin, K. J. Chin, D. G. Grenache, H. Bhatt, and S. M. Politz, 1991. Altered expression of an L1-specific, O-linked cuticle surface glycoprotein in mutants of the nematode *Caenorhabditis elegans*. *J. Cell Biol.* 115:1237–1247.

13. Johnson, K. L., 1985. Contact Mechanics. Cambridge University Press.

14. Camalet, S., F. Jülicher, and J. Prost, 1999. Self-organized beating and swimming of internally driven filaments. *Phys. Rev. Lett.* 82:1590–1593.

15. Wiggins, C. H., D. Riveline, A. Ott, and R. E. Goldstein, 1998. Trapping and wiggling: elastohydrodynamics of driven microfilaments. *Biophys. J.* 74:1043–1060.